Bioorganic & Medicinal Chemistry Letters 21 (2011) 3399–3403

Contents lists available at ScienceDirect

Bioorganic & Medicinal Chemistry Letters

journal homepage: www.elsevier.com/locate/bmcl

2,6-Disubstituted pyrazines and related analogs as NR2B site antagonists of the NMDA receptor with anti-depressant activity

Dean G. Brown [a,*], Donna L. Maier [a], Mark A. Sylvester [a], Tiffany N. Hoerter [a], Elnaz Menhaji-Klotz [a], Celina C. Lasota [a], Lee T. Hirata [a], Deidre E. Wilkins [a], Clay W. Scott [a], Shephali Trivedi [a], Tongming Chen [a], Dennis J. McCarthy [a], Carla M. Maciag [a], Evelynjeane J. Sutton [a], Jerry Cumberledge [a], Don Mathisen [a], John Roberts [a], Anshul Gupta [a], Frank Liu [a], Charles S. Elmore [a], Cristobal Alhambra [a], Jennifer R. Krumrine [a], Xia Wang [a], Paul J. Ciaccio [a], Michael W. Wood [a], James B. Campbell [a], Magnus J. Johansson [b], Jian Xia [c], Xiaotian Wen [c], Ji Jiang [c], Xiaoping Wang [c], Zuozhong Peng [c], Tao Hu [c], Jian Wang [c]

[a] CNS Discovery Research, AstraZeneca Pharmaceuticals, 1800 Concord Pike, Wilmington, DE 19850-5437, USA
[b] AstraZeneca R&D Mölndal, Pepparedsladen 1, SE-431 83, Mölndal, Sweden
[c] WuXi AppTec Co. Ltd, 288FuTe Zhong Road, WaiGaQiao Free Trade Zone, Shanghai 200131, PR China

ARTICLE INFO

Article history:
Received 23 February 2011
Revised 29 March 2011
Accepted 31 March 2011
Available online 8 April 2011

Keywords:
NMDA antagonist
NR2B
Anti-depressant

ABSTRACT

Herein we describe the discovery of compounds that are competitive antagonists of the CP101-606 binding site within the NR2B subtype of the NMDA receptor. The compounds identified do not possess phenolic functional groups such as those in ifenprodil and related analogs. Initial identification of hits in this series focused on a basic, secondary amine side chain which led to good potency, but also presented a hERG liability. Further modifications led to examples of non-basic replacements which demonstrated much less liability in this regard. Finally, one compound in the series, **6a**, was tested in the mouse forced swim depression assay and found to show activity (sc 60 mg/kg).

The *N*-methyl-D-aspartate receptor (NMDAr) is a ligand gated ion-channel which has been the target of multiple drug discovery efforts in the past two decades for a variety of indications including stroke, pain, and most recently depression.[1] Antagonists of the NMDA receptors are hypothesized to be useful therapeutic agents for the above indications based on the hypothesis that these pathological conditions involve a state of NMDA hyperfunction. However, it has been established that side effects such as ataxia and sedation are associated with NMDA anatagonists and have limited their clinical utility.[2] NMDA receptors have several different binding sites (ion channel, glutamate, glycine) as well as multiple subtypes (Eight NR1 eight splice variants and four NR2 subtypes A, B, C, and D).[3] At least one NR1 unit and one NR2 unit must be present to form the functional hetero-tetrameric receptor.[4] It has been speculated that selective antagonists of the NR2B subtype might provide a cleaner side effect profile.[5] With this in mind, we sought to identify structurally novel antagonists which provided potent activity at the NR2B subtype useful for treatment in depression.

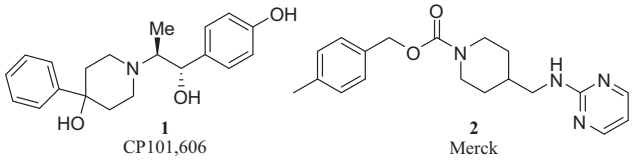

Figure 1. CP-101606 and Merck **2**.

One of the more advanced clinical compounds in this class is CP-101,606 **1** which has shown positive effects in a clinical study of major depressive disorder (Fig. 1).[6,7] These results have encouraged those in the field to look for other NMDA antagonist with improved drug-like properties. Historically, two key features in the early NR2B antagonists were phenols and basic amines. Within this series of compounds, the phenol can be problematic in metabolic clearance, whereas the basic amine can give rise to hERG and other issues such as potent CYP2D6 inhibition. In the more recent literature, NR2B antagonists have been reported that do not possess the phenolic moiety, or a basic amine such as **2** (Fig. 1).[8] It is hypothesized that both the basic amine and the phenol make contact with aspartic acid (Asp) residues in the binding pocket.[9]

* Corresponding author at present address: AstraZeneca Pharmaceuticals, 35 Gatehouse Drive, Waltham, MA 02451, USA.
E-mail address: dean.brown@astrazeneca.com (D.G. Brown).

0960-894X/$ - see front matter © 2011 Elsevier Ltd. All rights reserved.
doi:10.1016/j.bmcl.2011.03.117

Our effort to identify novel and selective NR2B antagonists relied on an iterative virtual screen using a rat brain binding assay with [^{3}H]CP101,606 as the ligand.[10] The principle of this assay selection was to help drive SAR, but also establish a correlation between binding and in vivo efficacy. The aim of the virtual screen was to identify key fragments outside of phenols that could interact with NR2B or other Asp containing receptors. A collection of known Asp containing fragments was generated by searching the literature as well as crystallographic databases. Using substructure searching, compounds were identified from our collection which contained these fragments as well as potential bio-isosteres of these fragments. The pool of potential screening compounds was narrowed down based on known and calculated physical properties (e.g., *c* log *P*, MW), and representatives of each cluster were selected. An initial group of approximately 1000 compounds was subsequently selected for single concentration testing. Actives with greater than 80% inhibition were followed up with concentration response testing. From this effort, an initial set of 80 actives was identified, which then served as the basis for another round of substructure searching and testing. Several more iterations of single concentration screening using sets of between 1000 to 2000 compounds were done using the same virtual screen protocol building on the newly identified actives with each cycle. The most promising actives were then followed up with IC_{50} measurements as well as physical property profiling, such as solubility and log *D*. Several new interesting scaffolds were identified, including the 2,6-disubstituted pyrazines as illustrated by **3** (Fig. 2).

Identification of these compounds prompted further exploration and synthetic expansion, the synthesis of which is illustrated in Schemes 1 and 2.

The synthesis of the 2,6-disubstituted pyrazines began with 2,3-dichloropyrazine, which was treated with one equivalent of *n*-BuLi, followed by trapping with 1,3-dithiane (Scheme 1).[11] The intermediate dithiane was then isolated and purified, followed by Suzuki coupling conditions to install the aromatic ring. The dithiane could then be removed to give the intermediate aldehyde, which was subsequently used in reductive amination reactions to yield target compounds **4a–r**.

To prepare analogs of the pyrazine scaffold, the general procedure in Scheme 2 was applied. Synthesis began with the commercially available halo-substituted aromatic/heteroaromatic aldehydes **5**, which were subjected to Suzuki coupling reactions, and then treated under reductive amination conditions identical to Scheme 1. As a variant to this, and in order to gain access to the primary amine, the aldehyde could be treated with hydroxylamine, and reduced under catalytic hydrogenation conditions (**7** and **8**). The resultant primary amine was then coupled with electrophiles such as acid chlorides to give **8** as an illustrative example.

Results for compounds **4a**–**r** are shown in Table 1. Through the course of the iterative virtual screen, it became apparent that a preferred substituted aromatic ring was the 2-MeO, 4-F phenyl ring. The 2,3-difluoro aromatic ring showed some activity but was not as potent as the 2-MeO, 4-F (e.g., **4a** vs **k**).

Replacement of the 4-F (**4c**) with 4-MeO led to a significant loss in activity (**4q**). Other substitutions such as 3-CN, 4-CN and were very weak or too weak to be determined in the assay.

At this stage in the project we choose to keep the 2-MeO, 4-F constant while investigating the SAR off the 6 position of the

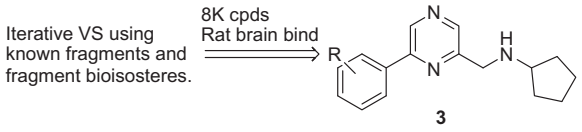

Figure 2. Virtual screen identifying 2,6-disubstituted pyrazines.

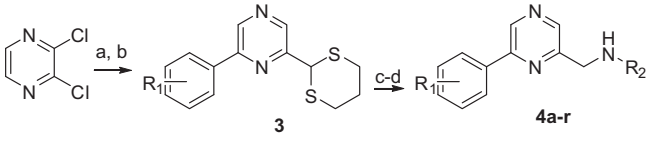

Scheme 1. Reagents and conditions: (a) *n*-BuLi, THF, 1,3-dithiane, −50 °C, 65%; (b) R_1-B(OH)$_2$, Pd(PPh$_3$)$_4$, K_2CO_3, EtOH, PhMe, 20–80%; (c) MeI, $CaCO_3$, acetone, H_2O, 60 °C, 96%; (d) R_2NH_2, $NaBH_3CN$, MeOH, 30–92%.

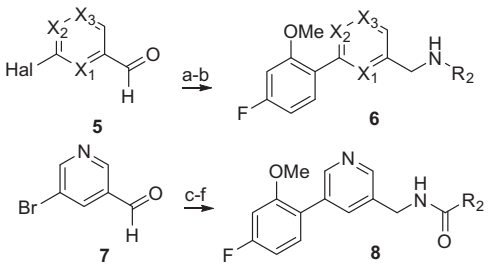

Scheme 2. Reagents and conditions: (a) R_1-B(OH)$_2$, Pd(PPh$_3$)$_4$, K_2CO_3, EtOH, PhMe, 25–80%; (b) R_2NH_2, $NaBH_3CN$, MeOH, 30–90%; (c) 2-MeO, 4-F-phenylboronic acid, DME, EtOH, H_2O, Cs_2CO_3, $PdCl_2$(dppf)-DCM, 62%; (d) NH_2OH, NaOAc, EtOH, 87%; (e) H_2, MeOH, HCl, Pd/C, 40 psi, 97%; (f) R_2COCl, TEA, DCM, 95%.

pyrazine. Small cycloalkyls such as CH_2-cyclopropyl (**4a**), cyclobutyl (**4b**) and cyclopentyl (**4c**) were the most potent compounds of the ones synthesized and tested.

Acyclic alkyls were typically 3- to 4-fold less potent than the cycloalkyls (**4d** and **e**). It is possible this is attributable to more optimal interactions in the hydrophobic pocket achieved by the larger cycloalkyl groups relative to straight chain analogs. A few attempts were made at this stage to incorporate more hydrophilic groups into the right hand side chain as a way of making hERG less potent, and, in this context, we explored 2-pyridyl (**4i**) and (*S*)-CH_2-2-THF (**4h**) as illustrative examples. These modifications led to a decrease in potency relative to small cycloalkyl groups.

We next turned our attention to core modifications using the preferred aromatic substitution pattern (2-MeO, 4-F) and a preferred right hand side amine (cyclopentyl, Table 2). The results show that potency can be achieved with different ring modifications such as pyridine isomer **6a**,[12] which was slightly more potent than the matched-pair pyrazine analog (**6a** = 12 nM vs **4c** = 54 nM). The pyridine nitrogen isomer **6c** led to a slight decrease (~4-fold) in potency. Synthesis of the third and final pyridine isomer **6d** led to a substantial loss in activity (>8 μM). We speculate that perhaps the MeO group and the pyridine lone pair create a repulsive force which twists the methoxy group out of a biologically relevant conformation. It also could be rationalized that a nitrogen lone pair in this position has an electronic mis-match in the receptor which leads to the significant loss in activity. Unfortunately crystallographic studies were not amenable to this target in order to further substantiate these hypotheses. Interestingly, replacement of the pyridine with a phenyl ring (**6b**) shows very little loss in activity relative to the pyrazine and pyridine cores. Although these core replacements shed light on the SAR and scope around the pyrazine core, they were inferior with respect to hERG when compared to the original pyrazine. It was presumed that the potent hERG activity of analogs **6a**, **b**, **c**, and **d** was most likely due to the lipophilic nature of these analogs as well as the presence of a strongly basic side chain.

With this in mind, we sought to explore modifications on the amine side chain using the most potent pyridine scaffold (**6a**) and the most potent aromatic ring substitution (2-MeO, 4-F). Results of this study are shown in Table 3. Among the modifications

Table 1
Scoping of pyrazine analogs

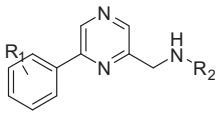

Entry	R1	R2	NR2B bind K_i[a] (nM)
1	—	—	4.6 (±1.2)
4a	2-OMe, 4-F	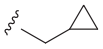	27 (±10)
4b	2-OMe, 4-F		53 (±27)
4c	2-OMe, 4-F		54 (±28)
4d	2-OMe, 4-F	$-(CH_2)_2OMe$	214 (±61)
4e	2-OMe, 4-F	$-CH_2CH(CH_3)_2$	217 (±65)
4f	2-OMe, 4-F	$-CH_2CH_3$	255 (±112)
4g	2-OMe, 4-F		429 (±66)
4h	2-OMe, 4-F		610 (±516)
4i	2-OMe, 4-F	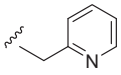	3565 (±100)
4j	2,3-di-F		186 (±84)
4k	2,3-di-F	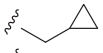	341 (±274)
4l	2,3-di-F		2979 (±600)
4m	2-F, 3-OMe	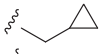	602 (±114)
4n	2-F, 3-OMe		5700 (±700)
4o	3-CN		1554 (±100)
4p	4-CN		1571 (±300)
4q	2-OMe, 4-OMe		1689 (±200)
4r	3-NHAc		>10 μM

[a] All values are the mean ± standard deviation of at least $n = 2$ experiments. Inhibition of binding of [^{3}H]CP101,606 to rat brain membranes.

Table 2
Core modifications

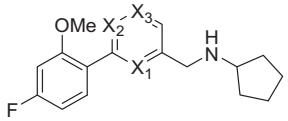

Entry	X1	X2	X3	NR2B bind K_i[a] (nM)	hERG IC_{50}[b] (μM)	*c* log *P*[c]
6a	C	C	N	12 (±6)	1.89	3.06
6b	C	C	C	48 (±9)	2.15	4.51
4c	N	C	N	54 (±28)	16.0	2.31
6c	N	C	C	66 (±8)	6.23	3.27
6d	C	N	C	8900 (±1700)	3.85	3.27

[a] Inhibition of binding of [^{3}H]CP101,606 to rat brain membranes. All values are the mean ± standard deviation of at least $n = 2$ experiments.
[b] Values determined in CHOK1-hERG cells using electrophysiological measurements
[c] Calculated log *P*. General procedure and spectral data for compound **6a** is reported in Ref. 12 as an illustrative example.

Table 3
Right hand side modifications

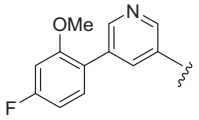

Entry	Side chain	NR2B bind K_i[a] (nM)	hERG IC_{50}[b] (μM)	*c* log *P*[c]
6e	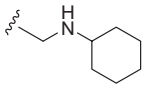	112 (±56)	2.18	3.61
6f	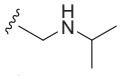	266 (±105)	6.67	2.42
6g		440 (±13)	8.62	2.01
6h	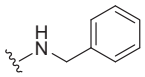	457 (±125)	5.2	2.74
6i	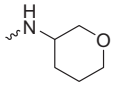	705 (±57)	9.4	2.01

[a] Inhibition of binding of [^{3}H]CP101,606 to rat brain membranes. All values are the mean ± standard deviation of at least $n = 2$ experiments.
[b] Values determined in CHOK1-hERG cells using electrophysiological measurements.
[c] Calculated log *P*.

explored, pyrrolidine **6g** served as a probe of conformational constraint of the secondary amine and was ~400-fold less active. It should however be noted, that inhibitory activity was still present even after this significant perturbation. Hydrophilic substitutions on the amine side chain such as tetrahydropyran **6i** typically also resulted in loss in potency. At this stage we did not see dramatic improvements in the hERG values relative to **6a** and sought to explore surrogates for the secondary amine itself (Table 4).

Based on a pharmacophore that evolved from the use of both internal and external homology models of NR2B,[9] we hypothesized that non-basic or less basic replacements of the secondary amine side chain (e.g., amides) could form a H-bond interaction with the targeted Asp residue while reducing hERG potency. The most potent aromatic substitution patterns (2-MeO, 4-F) and core scaffold (**6a**) were chosen to probe a variety of amide and urea side chains (Table 4). The most potent analog in this series was the 2-pyazine amide **8a**, which shows about 7-fold lower activity relative to **6a**. We were encouraged by these results considering significant activity was still observed even though what is typically considered a very strong protonated amine-Asp interaction between the ligand and receptor had been replaced. Pyridine analog **8b** was slightly less potent than pyrazine **8a**, but had more promising hERG values relative to **8a** and **6a**. (e.g., **4a** = 1.89 μM vs **8a** = 7.11 μM vs **8b** = 27 μM). The potency of the 2-pyridyl and 2-pyrazyl side chain analogs relative to the other analogs in the table suggests that the heteroatom in the 2-postion may pick up an additional interaction in the receptor, possibly the targeted Asp residue. It is also possible that the *ortho*-substituted heterocycle alters the H-bond character or desolvation energetic of the amide bond. Other substitutions suggest that it is possible to bring in a

Table 4
Replacements of secondary amines

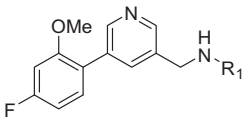

Entry	R1	NR2B bind K_i[a](nM)	hERG IC_{50}[b] (μM)	*c* log *P*[c]
8a	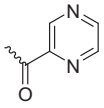	80 (±5)	7.11	1.72
8b	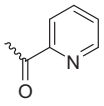	116 (±29)	27	2.50
8c	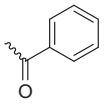	450 (±135)	18.8	2.90
8d	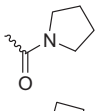	268 (±20)	Nt[d]	1.98
8e	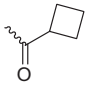	340 (±37)	18.6	1.94
8f	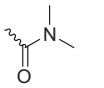	420 (±72)	Nt[d]	1.19
8g	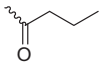	468 (±89)	Nt[d]	2.08
8h	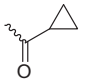	595 (±56)	>33	1.61
8i	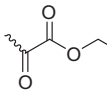	778 (±136)	Nt[d]	1.41

[a] Inhibition of binding of [^{3}H]CP101,606 to rat brain membranes. All values are the mean ± standard deviation of at least $n = 2$ experiments.
[b] Values determined in CHOK1-hERG cells using electrophysiological measurements.
[c] Calculated log *P*.
[d] Not tested.

variety of functional groups (e.g., **8c**, **d**, and **i**) while keeping the binding potency below 1 μM.

Several of the more potent compounds were characterized in an NR2B functional antagonist assay using over-expressed human receptors[13] as well as selected in vitro DMPK assays (Table 5). Although the functional assay did correlate with the binding assay in a relative sense, the functional assay demonstrated typically 1–2 log units less potency than the binding assay. We examined a few possibilities of this disconnect, (e.g., rat vs human and native vs recombinant receptor), but were unable to determine the root cause. Nonetheless, the assay served as a useful indicator of functional antagonism at the human receptor. All compounds tested also demonstrated good aqueous solubility,[14] and low human metabolic clearance in an in vitro microsomal clearance assay (Table 5).

One major difference that emerged between the secondary amine and secondary amide analogs was inhibition of the CYP2D6 isoform. Potent inhibition discriminated secondary amines from the secondary amide side chains. The amide replacements of the secondary amine **8a** and **8b** showed dramatic improvements in CYP2D6 inhibition..

Several compounds were evaluated in an NR2A oocyte assay to determine NR2B selectivity. Typically non-selective NMDA antagonists such as channel blockers, glutamate antagonists, and glycine-site antagonists show very little difference between the sub-types, and would be expected to show equipotent activity in assays expressing only single sub-units. Compounds **6a**, **b**, **4b**, **6c**, **8c** and CP101-606 (**1**) were tested in this assay and showed no activity below 90 μM (limits of detection of the assay).[15] By comparison, MK-801 (non-selective channel blocker) had an IC_{50} value of 29 nM.

The most potent example in the series (**6a**) was further evaluated in mouse forced swim model of depression (Table 6).[16] Doses of 10, 30 and 60 mg/kg were evaluated (sc dosing) and compared to the known standard Imipramine (sc 20 mg/kg). Compound **6a** was active in this model at 60 mg/kg. Samples were taken at 0.5 h post-dose and analyzed for plasma and brain concentrations. Exposure to **6a** increased in an approximate dose-proportional manner in both plasma and brain tissue across the dose range tested with a brain to plasma ratio of 10. Compound **6a** was also examined in a mouse locomotion assay at a single dose of 60 mg/kg in order to determine if the effects were simply due to reduced mobility. The mouse was monitored for any abnormal movements following the administration of the test compound. The compound did not show any effect at this dose thus supporting that the compound is working as an anti-depressant and not a general sedative. Although the in vivo efficacy in the mouse forced swim is not as potent as the standard imipramine, it was felt that with further optimization of **6a** greater in vivo efficacies can be achieved.

In summary, a new class of NR2B antagonists has been identified using an iterative virtual screen, and subsequently characterized using in vitro pharmacology as well as in vitro ADME assays. Evolution of the original secondary amine side chain into the amide side chain resulted in a loss of potency, but did improve hERG and CYP2D6. In vivo characterization of compound **6a** demonstrated plasma and brain exposure along with activity in the mouse forced swim model of depression (sc 60 mg/kg). It is our hope that further optimization of these compounds will lead to

Table 5
Characterization of leading compounds

Entry	hNR2B fxn (nM)[a]	Sol (μM)[b]	hClint [c]	CYP2D6[d] (IC_{50} μM)	CYP3A4[e] (IC_{50} μM)
6a	770 (±73)	>450	74	0.23	>20
4a	508 (±12)	340	108	0.38	>20
8a	262 (±55)	63	64	>20	>20
8b	673(±62)	200	45	>20	>20
1	74 (±15)	>470	37	4.25	>20

[a] IC_{50} values. See Ref. 13.
[b] Equilibrium solubility (pH 7.4). See Ref. 12.
[c] Human liver microsomal clearance expressed as μL/min/mg.
[d,e] Cytochrome P450 inhibition of 2D6 and 3A4 subtypes.

Table 6
In vivo characterization of **6a** in mouse forced swim assay

Dose of compd **6a**	Immobility time[a]	Plasma concn[b] (nM)	Brain concn[b] (nmol/kg)	Brain/plasma ratio
10 mg/kg	100.89 (±11.16)	867 (±195)	9671 (±3073)	10.9
30 mg/kg	97.33 (±9.50)	2321 (±767)	32375 (±13173)	13.6
60 mg/kg	59.00*(±9.45)	3372 (±1326)	44158 (±23092)	12.6
Imipramine[c]	51.36**(±9.50)	Nm[d]	Nm[d]	Nm[d]

[a] Time measured of mice 30 min post doing.
[b] Plasma and brain samples were collected at 0.5 h post dosing.
[c] 20 mg/kg sc.
[d] Not measured.
* $p < 0.05$ is associated with *t*-test comparing imipramine versus control.
** $p < 0.01$ is associated with one-way ANOVA comparing imipramine versus control.

more potent examples, while maintaining some of the positive drug-like features.

References and notes

1For stroke see: Lee, J.-M.; Zipel, G. J.; Choi, D. W. *Nature* **1999**, *399*, A7; For pain see: (b) Brown, D. G.; Krupp, J. J. *Curr. Top. Med. Chem.* **2006**, *6*(8), 749; For depression see: (c) Skolnick, P.; Popik, P.; Trullas, R. *Trends Pharm. Sci.* **2009**, *30*(11), 563.
2. (a) Kemp, J. A.; McKennan, R. M. *Nat. Neurosci.* **2002**, *5*, 1039; (b) Paoletti, P.; Neyton *J. Curr. Opin. Pharmacol.* **2007**, *7*, 39.
3. Chizh, B. A.; Headley, P. M. *Curr. Pharm. Des.* **2005**, *11*, 2977.
4. Dingledine, R.; Borges, K.; Bowe, D.; Traynelis, S. F. *Pharmacol. Rev.* **1999**, *51*, 7.
5. Boyce, S.; Wyatt, A.; Webb, J. K.; O'Donnell, R.; Mason, G.; Rigby, M.; Sirinathsinghi, D.; Hill, R. G.; Rupinak, N. M. J. *Neuropharmacology* **1999**, *38*, 611.
6. For a review on the evolution of ifenprodil structures see: Layton, M. E.; Kelly, M. J., III; Rodzinak, K. J. *Curr. Top. Med. Chem.* **2006**, *6*(7), 697.
7. Preskorn, S. H.; Baker, B.; Kolluri, S.; Menniti, F. S.; Krams, M.; Landen, J. W. *J. Clin. Psychopharm.* **2008**, *28*(6), 631.
8. Liverton, N. J.; Bednar, R. A.; Bednar, B.; Buthcer, J. W.; Claiborne, C. F.; Claremon, D. A.; Cummingham, M.; DiLella, A. G.; Gaul, S. L.; Libby, B. E.; Lyle, E. A.; Lynch, J. J.; McCauley, J. A.; Mosser, S. D.; Nguyen, K. T.; Stump, G. L.; Sun, H.; Wang, H.; Yergey, J.; Koblan, K. S. *J. Med. Chem.* **2007**, *50*, 807.
9. For a recent paper on NR2B homology models see: Marinelli, L.; Cosconati, S.; Steinbrecher, T.; Limongelli, V.; Bertamino, A.; Novellino, E.; Case David, A. *ChemMedChem* **2007**, *2*(10), 1498.
10. The NR2B binding assay measured the IC_{50} of test compounds for displacing [^{3}H]CP101,606 binding to membranes from post-natal day 11 rat brain minus cerebellum. This was a filtration assay conducted in 96 well plate format. The assay was conducted in either single concentration or concentration effect mode. Compounds were solubilized in DMSO and tested in a final DMSO concentration of 1%.
11. Torr, J. E.; Large, J. M.; Horton, P. N.; Hursthouse, M. B.; McDonald, E. *Tetrahedron Lett.* **2006**, *47*, 31.
12. *Synthesis of* **6a**: 5-bromonicotinaldehyde (1.80 g, 9.67 mmol) was dissolved in DME/EtOH/H_2O (7:2:1, 1 M, 10 mL) and treated with 4-fluoro-2-methoxyphenylboronic acid (1.64 g, 9.67 mmol) followed by cesium carbonate (3.43 g, 10.54 mmol) and $PdCl_2$(dppf)-CH_2Cl_2 (0.32 g, 0.39 mmol). The reaction mixture was heated at 80 °C for 12 h and then partitioned between EtOAc and H_2O. The organic layer was washed with saturated $NaHCO_3$, saturated NaCl, dried over $MgSO_4$, filtered and concentrated under reduced pressure to give a dark brown solid. Chromatography (SiO_2, 0–50% ethyl acetate in hexanes) yielded the desired product as a white solid (1.38 g, 62% yield). ^{1}H NMR (300 MHz, $CDCl_3$-*d*) δ ppm 3.83 (s, 3 H) 6.66–6.91 (m, 2 H) 7.19–7.40 (m, 1 H) 8.26 (t, *J* = 2.11 Hz, 1 H) 9.00 (d, *J* = 2.11 Hz, 1 H) 8.94 (d, *J* = 2.32 Hz, 1 H) 10.17 (s, 1 H); *m*/*z* (ES+) M+1 = 231. The resultant aldehyde (0.300 g, 1.29 mmol) was dissolved in dichloromethane (3 mL) along with cyclopentyl amine (0.166 g, 0.192 mL, 1.94 mmol). The solution was cooled in an ice bath, and to this was added sodium triacetoxy borohydride (0.310 g, 1.50 mmol). The reaction was stirred at room temperature for 16 h and diluted with dichloromethane (50 mL). The resultant mixture was then washed with saturated $NaHCO_3$ (1 × 20 mL) and brine (1 × 20 mL). The combined organics were concentrated, and the residual oil purified by SiO_2 chromatography (0–5% MeOH/DCM) to give **6a** as a yellow oil. (0.12 g, 31%). NMR ^{1}H NMR (500 MHz, DMSO-d_6) δ ppm 1.35 (dt, *J* = 12.21, 6.41 Hz, 2 H) 1.45 (td, *J* = 7.17, 3.66 Hz, 2 H) 1.53–1.75 (m, 4 H) 3.00 (t, *J* = 6.26 Hz, 1 H) 3.28 (br s, 1 H) 3.73 (s, 2 H) 3.76–3.82 (m, 3 H) 6.89 (td, *J* = 8.39, 2.44 Hz, 1 H) 7.06 (dd, *J* = 11.29, 2.44 Hz, 1 H) 7.37 (dd, *J* = 8.39, 6.87 Hz, 1 H) 7.78 (t, *J* = 1.98 Hz, 1 H) 8.45 (d, *J* = 1.53 Hz, 1 H) 8.49 (d, *J* = 2.14 Hz, 1 H); *m*/*z* (TOF) (M+H) calcd = 301.1711 found = 301.1729.
13. The NR2B functional assay utilized the ChanTest NR1/NR2B HEK293 cell line. The cells were treated with tetracycline in the presence of ketamine in order to induce stable expression. Activation of the NR2B receptor with glutamate and glycine resulted in changes in cellular calcium concentrations that were quantified using a calcium sensitive dye and fluorescent detection platform.
14. Alelyunas, Y. W.; Liu, R.; Pelosi-Kilby, L.; Shen, C. *Eur. J. Pharm. Sci.* **2009**, *37*, 172.
15. The assay for NR2A activity employed stably transfected oocytes with NR1/NR2A receptors. Cells were stimulated with glutamate and glycine, and concentration response curves were determined by TEVC using OpusExpress 6000.
16. Porsolt, R. D.; Bertin, A.; Jalfre, M. *Nature* **1977**, *266*, 730. Mouse forced swim test is a widely accepted assay for anti-depressant effects. Mice are individually forced to swim in a container for a defined time interval. Immobility time is the amount of time the animal stops swimming and remains motionless in the water. A decrease in immobility time is a signature of an anti-depressant effect.